

## SUPPORTING INFORMATION

---

### Supporting Information

#### **Enabling ultra-specific lysosomal polarity fluorescence response via intramolecular $\pi$ - $\pi$ stacking-mediated conformational locking**

Jiaqi Su,<sup>a†</sup> Chunbai Xiang,<sup>a†</sup> Jiao Lu,<sup>b</sup> Binhao Li,<sup>a</sup> Yuxuan Liu,<sup>a</sup> Chuanhao Liu,<sup>c</sup> Shiyi Tian,<sup>a</sup> Wenxiao Deng,<sup>a</sup> Yuchang Tan,<sup>a</sup> Yanju Luo,<sup>c</sup> Yan Huang,<sup>a</sup> Yanfei Tan<sup>b\*</sup>, and Zhiyun Lu<sup>a\*</sup>

a. College of Chemistry, Sichuan University, Chengdu 610064, People's Republic of China. E-mail:

luzhiyun@scu.edu.cn.

b. National Engineering Research Center for Biomaterials and College of Biomedical Engineering, Sichuan

University, Chengdu, 610064 (P. R. China). E-mail: tanyf@scu.edu.cn.

### Contents

<b>1. Experimental procedures .....</b>	<b>3</b>
<b>1.1 General information. ....</b>	<b>3</b>
<b>1.2 Synthesis of P-DOTPA .....</b>	<b>5</b>
<b>2. Summary of Lysosomal Polarity Probes.....</b>	<b>7</b>
<b>3. Theoretical calculation .....</b>	<b>8</b>
<b>4. Photophysical characterization.....</b>	<b>9</b>
<b>5. Biological experiments.....</b>	<b>17</b>
<b>6. <sup>1</sup>H NMR, <sup>13</sup>C NMR, and HRMS .....</b>	<b>18</b>
<b>References .....</b>	<b>21</b>

## 1. Experimental procedures

### 1.1 General information.

**Materials.** Unless stated otherwise, all reagents and anhydrous solvents were purchased from *Bidepharm Ltd. Co.*, *Energy Chemical Co.* or *J&K Scientific Ltd. Co.* All solvents used in photophysical measurements were of analytical grade and freshly distilled before use. For 1,4-dioxane, prior to distillation, it was refluxed in the presence of sodium and benzophenone until dark blue; for other solvents, prior to distillation, activated 4Å molecular sieves were added and stored for more than 48 hours with frequent shaking. Dulbecco's modified Eagle's medium (DMEM), phosphate-buffered saline (PBS), fetal bovine serum (FBS) and Buffer solutions (PH = 1-13) were purchased from Grand Island Biological Compan. Mitochondrial tracker, endoplasmic reticulum tracker, nucleus tracker and lysosomal tracker were purchased from Shanghai Biyuntian Biotechnology Co., Ltd. The ROS detection kit (DCFH probe) was purchased from Shanghai Macklin Biochemical Technology Co., Ltd.

**Measurement and Instruments.**  $^1\text{H}$  NMR and  $^{13}\text{C}$  NMR spectra were acquired on a Bruker AVANCE II-400 MHz spectrometer at 400 and 100 MHz in  $\text{CDCl}_3$ , respectively. Tetramethylsilane (TMS) was utilized as an internal standard. High-resolution MS spectra were obtained via a QTOF Premier ESI mass spectrometer (Micromass, Manchester, UK). UV-visible spectra were recorded using a HITACHI U-2910 spectrophotometer. Steady-state photoluminescence (PL) at room temperature (RT) measurements were conducted on a Horiba Jobin Yvon FluoroMax fluorescence spectrophotometer. PL decay profiles were measured by a time-correlated single-photon counting (TCSPC) system using a HORIBA Jobin Yvon Fluorolog-3 fluorescence spectrometer. The concentration of solution samples for photophysical measurements was  $1 \times 10^{-5} \text{ mol}\cdot\text{L}^{-1}$ . Cellular imaging experiments were performed with a confocal laser scanning microscope (LSM 900 with Airyscan2, Zeiss, Germany).

**Computational Methods Details.** The geometries of P-DOTPA in both the ground state ( $S_0$ ) and excited state ( $S_1$ ) were optimized at the density functional theory (DFT) level using the B3LYP hybrid functional and the 6-31G(d) basis set. Additionally, the root mean square deviation (RMSD), the reduced density gradient (RDG) scatter diagrams, and the RDG isosurface map were calculated as part of this optimization process.

**Determination of Fluorescence Quantum Yields.** The quantum yields of **P-DOTPA** were determined using the dye Rhodamine B, (10  $\mu\text{M}$ ,  $\Phi_r = 0.69\%$ , in 75% ethyl alcohol)<sup>[2]</sup> as a reference. The quantum yields were calculated as follows:

$$\varphi_x = \varphi_s \times \left(\frac{I_x}{I_s}\right) \times \left(\frac{F_s}{F_x}\right) \times \left(\frac{n_x}{n_s}\right)^2$$

## SUPPORTING INFORMATION

Among them,  $\Phi$  is the fluorescence quantum yield of the solution;  $F$  is the integral area of the fluorescence emission spectrum obtained by the solution under the corresponding excitation wavelength;  $A$  is the ultraviolet absorption of the solution under the maximum ultraviolet absorption wavelength ( $\leq 0.05$ );  $\lambda_{\text{ex}}$  is the excitation wavelength;  $n$  is the relative refractive index of the solution, and the subscripts  $x$  and  $s$  refer to the unknown and the standard, respectively.

**Total ROS detection.** DCFH was used to assess the reactive oxygen species (ROS) generation of chemicals. The DCFH solution was prepared by hydrolyzing DCFH-DA in an alkaline solution. DCFH-DA solution (0.25 mL, 0.5 mg/mL) was added to NaOH solution (1 mL, 10 mM) and incubated for 30 min in the dark. Afterward, the resultant solution was added to PBS (50 mM, 5 mL) to obtain the DCFH solution (40  $\mu\text{M}$ ). For ROS detection, DCFH solution (40  $\mu\text{M}$ , 200  $\mu\text{L}$ ) was added to the solution obtained from the chemicals in PBS (800  $\mu\text{L}$ ). The mixture containing **P-DOTPA** was subjected to light irradiation (250 mW/cm<sup>2</sup>) for various periods. The fluorescence emission of DCFH at 500-600 nm was recorded to determine the ROS generation rate. As a control, the DCFH solution without chemicals was subjected to irradiation. The response process of the general reactive oxygen species (ROS) probe DCFH: Reactive oxygen species (ROS) can oxidize the non-fluorescent DCFH into 2',7'-dichlorofluorescein (DCF), which is fluorescent. This process activates DCFH, producing a green fluorescent signal. The intensity of the fluorescent signal is proportional to the levels of ROS within the cells. Therefore, by detecting the fluorescence intensity of DCF, one can analyze the ROS content in the cells.

**O<sub>2</sub><sup>-•</sup> detection.** DHR 123 was used as the superoxide radical indicator. The cuvette containing a mixture of DHR 123 and **P-DOTPA** was subjected to light irradiation (250 mW/cm<sup>2</sup>) for various durations, and the fluorescence emission of DHR 123 at 500-600 nm was recorded after each irradiation. The DHR 123 solution without chemicals was used as a control during irradiation.

**<sup>1</sup>O<sub>2</sub> detection.** ABDA (50  $\mu\text{M}$ ) was utilized as a <sup>1</sup>O<sub>2</sub> indicator to detect the generation of <sup>1</sup>O<sub>2</sub> from chemicals. The cuvette containing a mixture of ABDA and **P-DOTPA** was irradiated with light (250 mW/cm<sup>2</sup>) for various times, and the decrease in ABDA was monitored by the absorbance at 378 nm. As a control, the ABDA solution without chemicals was subjected to irradiation.

**Cell Culture.** All the cell lines were kindly provided by National Research Center for Biomaterials, Sichuan University. 4T1 and CHO cells were cultured in DMEM medium supplemented with 10% fetal bovine serum and 1% antibiotics at 37 °C and 5% CO<sub>2</sub>.

**Cell viability assay.** The cell cytotoxicity of **P-DOTPA** to living 4T1 cells was assessed using a standard CCK-8 assay (cell counting kit-8). About  $1 \times 10^4$  cells/well in 100  $\mu\text{L}$  cell culture medium were seeded in a 96-well microplate. The medium was then replaced with fresh medium containing **P-DOTPA** at various concentrations of 0  $\mu\text{M}$ , 2.5  $\mu\text{M}$ , 5  $\mu\text{M}$ , 10  $\mu\text{M}$ , and 15  $\mu\text{M}$  for 24 h. Subsequently, the cells were washed with fresh medium three times, and 10  $\mu\text{L}$  CCK-8 in 90  $\mu\text{L}$  PBS was added to each well for another 1 h. The absorbance was measured using an ELISA microplate reader at a wavelength of 450 nm.

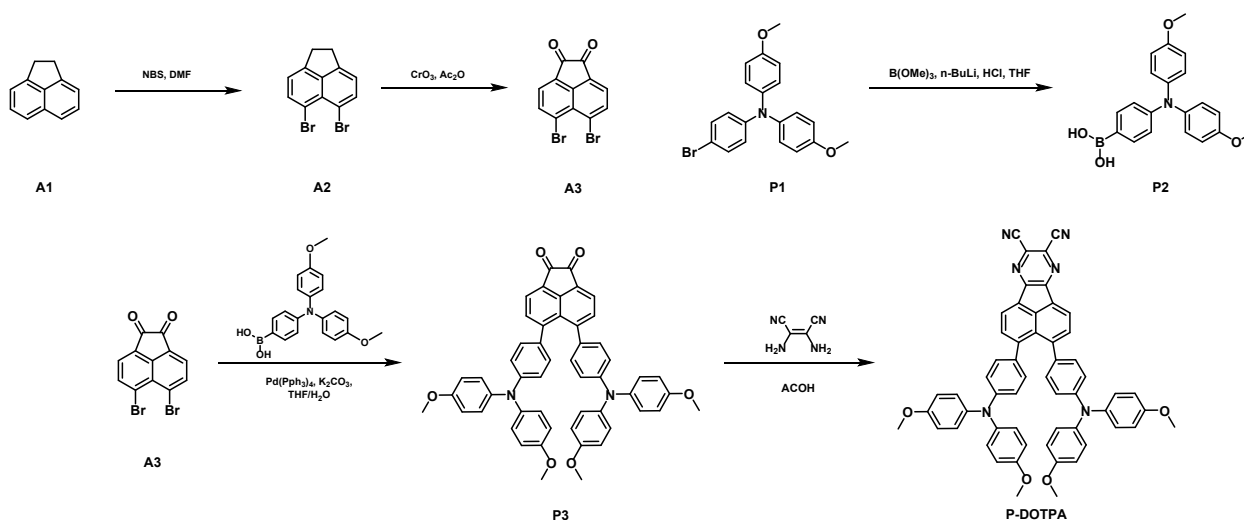
## SUPPORTING INFORMATION

Cell viability was expressed relative to the control group, which was considered to have 100% metabolic activity.

**Subcellular localization Study.** 4T1 cells were seeded on a confocal dish with  $1 \times 10^4$  cells per dish and 1 mL medium overnight. Then, 4T1 cells were incubated with culture medium containing **P-DOTPA** (10  $\mu$ M) for 4.5 h. After that, the medium was removed, and the cells were washed 3 times with PBS. The cells were then stained with Lyso Tracker, Mito Tracker, and ER Tracker, and also stained with Hoechst 33342 for the nuclei. Fluorescence images were obtained by CLSM under different parameters (Lyso-Tracker,  $\lambda_{\text{ex}}/\lambda_{\text{em}} = 488/500\text{--}600$  nm; ER-Tracker,  $\lambda_{\text{ex}}/\lambda_{\text{em}} = 488/500\text{--}600$  nm; Nucleus-Tracker,  $\lambda_{\text{ex}}/\lambda_{\text{em}} = 405/420\text{--}500$  nm; Mito-Tracker,  $\lambda_{\text{ex}}/\lambda_{\text{em}} = 488/500\text{--}600$  nm; for **P-DOTPA**,  $\lambda_{\text{ex}}/\lambda_{\text{em}} = 561/600\text{--}850$  nm).

**Determination of Intracellular ROS.** The ROS production of **P-DOTPA** was assessed under conditions of 37 °C and 5% CO<sub>2</sub>, and determined by a ROS detection kit (DCFH-DA probe). 4T1 cells were seeded into a 6-well plate until they reached a density of about 80%, and then the cells were incubated with **P-DOTPA** (10  $\mu$ M). After 4.5 h of incubation, the medium of these cells was replaced with fresh medium containing 20  $\mu$ M DCFH probe for 30 minutes. After washing, the cells were exposed to white laser irradiation (250 mW/cm<sup>2</sup>) for 5 minutes, and the fluorescent signal was collected from 510-600 nm (green; excitation: 488 nm) using CLSM. Four groups (PBS, PBS+Light, **P-DOTPA**) served as controls, which were performed with the same steps.

### 1.2 Synthesis of P-DOTPA



Scheme S1. The synthetical routs of **P-DOTPA**.

#### 5,6-Dibromo-1,2-dihydroacenaphthylene (A2)

A stirred suspension of acenaphthene (40.0 g, 259 mmol) in dry DMF (250 mL) was cooled to 0 °C. Over the course of 3 hours, NBS (115 g, 648 mmol) was added in portions. After an additional two hours of stirring, the temperature was raised to 10 °C, and the suspension was stirred overnight. The

## SUPPORTING INFORMATION

cooled mixture was filtered to yield a crude colourless product, which was purified by recrystallization from a mixture of  $\text{CHCl}_3$  and MeOH. Compound A2 (8.39 g, 26.9 mmol, 10%) was obtained as colourless crystals.  $^1\text{H}$  NMR (400 MHz,  $\text{CDCl}_3$ )  $\delta$  (ppm): 7.80 (d,  $J = 7.6$  Hz, 2H), 7.10 (d,  $J = 7.6$  Hz, 2H), 3.31 (s, 4H) ppm.

### 5,6-Dibromoacenaphthylene-1,2-dione (A3)

A 20 mL reaction tube was combined with A2 (50.0 mg, 160  $\mu\text{mol}$ ) and  $\text{Ac}_2\text{O}$  (5.00 mL). The tube was warmed to 110  $^\circ\text{C}$  until the starting material was fully dissolved. Chromium(VI) oxide (160 mg, 1.60 mmol) was added in portions over a period of 30 min, and the reaction mixture was heated to 160  $^\circ\text{C}$  for 1.5 h. The reaction mixture was filtered through a pad of hot sand, and the filtrate was cooled to 7  $^\circ\text{C}$ . After filtration, compound A3 (53.2 mg, 156  $\mu\text{mol}$ , 98%) was obtained as an orange solid.  $^1\text{H}$  NMR (400 MHz,  $\text{CDCl}_3$ )  $\delta$  (ppm): 8.26 (d,  $J = 7.6$  Hz, 2H), 7.93 (d,  $J = 7.6$  Hz, 2H) ppm.

### 4-(Bis(4-methoxyphenyl) amino) phenylboronic acid (P2).

To a 100 mL two-necked flask containing the solution of compound P1 (7.14 g, 22 mmol) in dried THF (20 mL), equipped with a magnetic stirrer, an  $\text{N}_2$  purge, and a  $-78$   $^\circ\text{C}$  acetone dry ice bath,  $n\text{-BuLi}$  (17.6 mL, 26.4 mmol, 1.5 M) was added dropwise while maintaining stirring. After stirring for 1 h, trimethyl borate (3.00 mL, 26.4 mmol) was carefully added. After stirring at room temperature for an additional 2 h, water was first added to the reaction mixture and then  $\text{HCl}$  (6 M) was added in a dropwise fashion until an acidic mixture was formed. The reaction mixture was poured into water and extracted with  $\text{CH}_2\text{Cl}_2$  ( $3 \times 50$  mL). The combined organic layer was dried with anhydrous  $\text{Na}_2\text{SO}_4$  and evaporated to dryness. The crude product was purified by column chromatography using  $\text{CH}_2\text{Cl}_2$ : ethyl acetate (v: v, 1: 1) as the eluent. The boronic acid compound P2 was obtained as a white solid with an isolated yield of 77%.  $^1\text{H}$  NMR (400 MHz,  $\text{CDCl}_3$ )  $\delta$  (ppm):  $\delta$  7.95 (d,  $J = 8.8$  Hz 2H), 7.12 (d,  $J = 8.8$  Hz, 4H), 6.93 (d,  $J = 8.4$  Hz, 2H), 6.88-6.84 (d,  $J = 8.8$  Hz 4H), 3.81 (s, 6H).

### 5,6-bis(4-(bis(4-methoxyphenyl) amino) phenyl) acenaphthylene-1,2-dione (P3).

Compound A3 (2.00 g, 5.80 mmol), P2 (4.19 g, 12.00 mmol), and  $\text{Pd(PPh}_3)_4$  (0.46 g, 0.40 mmol) were dissolved in THF (130 mL) under an argon atmosphere. After stirring the resultant mixture at 50  $^\circ\text{C}$  for 10 min, 30 mL of degassed 2 M  $\text{Na}_2\text{CO}_3$  aqueous was added, and then the mixture was heated to reflux overnight. The reaction mixture was cooled to room temperature, and the solvent was removed under reduced pressure. The crude product was dissolved in 120 mL of dichloromethane and washed with water. The organic layer was dried over anhydrous  $\text{Na}_2\text{SO}_4$  and concentrated by rotary evaporation. The remaining solid was purified by column chromatography using petroleum ether/dichloromethane (1/3) as the eluent to give 2.89 g of a red solid in 63% yield.  $^1\text{H}$  NMR (400 MHz,  $\text{CDCl}_3$ )  $\delta$  (ppm): 8.15 (d,  $J = 7.2$  Hz, 2H), 7.76 (d,  $J = 7.2$  Hz, 2H), 7.12 (d,  $J = 8.8$  Hz, 8H), 6.85-6.80 (m, 12H), 6.73 (t,  $J = 8.8$  Hz, 4H), 3.8 (s, 12H).

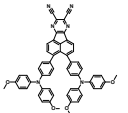
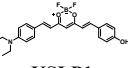
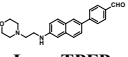
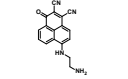
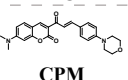
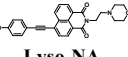
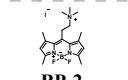
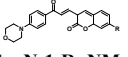
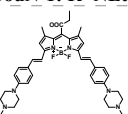
## SUPPORTING INFORMATION

### 3,4-bis(4-(bis(4-methoxyphenyl)amino)phenyl)acenaphtho[1,2-b]pyrazine-8,9-dicarbonitrile(P-DOTPA)

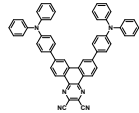
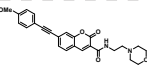
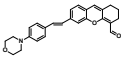
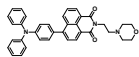
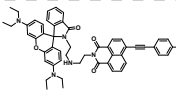
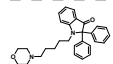
Compound P3 (2.05 g, 2.60 mmol) and 2,3-diaminomaleonitrile (0.56 g, 5.20 mmol) were added to 50 mL of glacial acetic acid, and then the suspension was refluxed overnight under an argon atmosphere. After cooling to room temperature, the mixture was poured into 200 mL of water. The separated solid was filtered, washed with water, cooled with methanol ice, and then dried under a vacuum. The crude product was purified by column chromatography (silica gel) using petroleum ether/dichloromethane (1/1, v/v) as the eluent. A dark purple solid was finally obtained after it was stirred in refluxing ethanol, followed by filtration and drying in a vacuum. Yield: 1.84 g (89%). This compound was further purified by sublimation prior to its application.  $^1\text{H}$  NMR (400 MHz,  $\text{CDCl}_3$ )  $\delta$  (ppm): 8.52 (d,  $J = 7.4$  Hz, 2H), 7.86 (d,  $J = 7.4$  Hz, 2H), 7.12 (d,  $J = 8.9$  Hz, 8H), 6.92 (d,  $J = 8.6$  Hz, 4H), 6.82 (d,  $J = 8.8$  Hz, 8H), 6.76 (d,  $J = 8.7$  Hz, 4H), 3.80 (s, 12H).  $^{13}\text{C}$  NMR (100 MHz,  $\text{CDCl}_3$ )  $\delta$  (ppm): 171.1, 156.1, 153.7, 148.5, 147.9, 140.3, 137.7, 132.2, 130.9, 129.2, 126.9, 126.6, 125.6, 118.7, 114.8, 114.4, 60.4, 55.5. HRMS (ESI)  $m/z$  calcd for  $\text{C}_{55}\text{H}_{40}\text{N}_6\text{O}_4$   $[\text{M} + \text{H}]^+$  861.3184, found: 861.3186.

## 2. Summary of Lysosomal Polarity Probes

**Table S1.** Comparison of Lysosome polarity fluorescent probes.

Emitter	$\lambda_{\text{abs}}$ (nm)	$\lambda_{\text{em}}$ (nm)	PLQY	$\Delta f_{\text{slope}}$	$E_{\text{T}}(30)_{\text{slope}}$	Reference
 <b>P-DOTPA</b>	505-650	755-908	23.5%	$\Delta f\text{-}\lambda_{\text{F}}: 418.0$ $\Delta f\text{-}I_{\text{F}}: -9.1 \times 10^7$	$E_{\text{T}}(30)\text{-}\lambda_{\text{F}}: 30.2$	This work
 <b>KSLP1</b>	552	612	/	$\Delta f\text{-}I_{\text{F}}: -1 \times 10^3$	/	[3]
 <b>Lyso-TPFP</b>	362	458	44%	/	$E_{\text{T}}(30)\text{-}\lambda_{\text{F}}: 12.0$	[4]
 <b>DC</b>	565	580,600	/	$\Delta f\text{-}\lambda_{\text{F}}: 7.0$	/	[5]
 <b>CPM</b>	453	550	25%	$\Delta f\text{-}I_{\text{F}}: -3.7 \times 10^6$	/	[6]
 <b>Lyso-NA</b>	398	460	/	$\Delta f\text{-}I_{\text{F}}: -2.6 \times 10^4$	/	[7]
 <b>BP-2</b>	510	523	4%	$\Delta f\text{-}I_{\text{F}}: 7.2$	/	[8]
 <b>CouN-1: R=NMe<sub>2</sub></b> <b>CouN-1: R=NEt<sub>2</sub></b>	465 472	568 560	0.26% 0.92%	$\Delta f\text{-}I_{\text{F}}: -1 \times 10^6$	/	[9]
 <b>SNL</b>	700	755	49%	$\Delta f\text{-}I_{\text{F}}: -899.8$	$E_{\text{T}}(30)\text{-}\lambda_{\text{F}}: 3.4$	[10]

## SUPPORTING INFORMATION

	450	688	/	$\Delta f-\lambda_F$ : 1016.9 $\Delta f-I_F$ : $3.1 \times 10^7$	/	[11]
<b>TPA-DCPP</b>						
	375	500	/	$\Delta f-I_F$ : 16028.0	/	[12]
<b>Lyso-OC</b>						
	427	529	83%	/	$E_T(30)-\lambda_F$ : 11.7	[13]
<b>LD-H-Lyso</b>						
	411	537	30.8%	/	$E_T(30)-\lambda_F$ : 9.4	[14]
<b>MND-Lys</b>						
	399	493	/	$\Delta f-I_F$ : -9254.9	/	[15]
<b>Lyso-NRB</b>						
	429	451	32%	/	$E_T(30)-\lambda_F$ : 8.2	[16]
<b>LyPol</b>						

### 3. Theoretical calculation

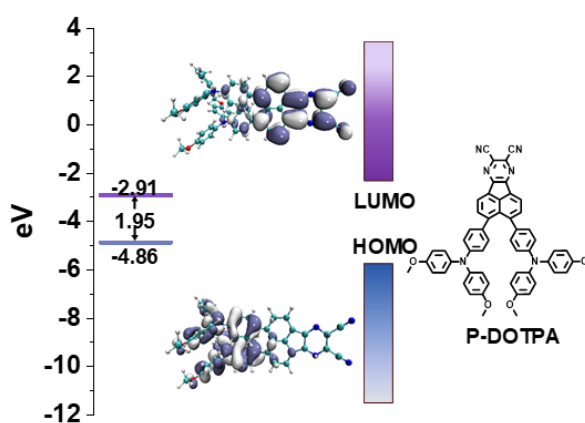


**Figure S1.** HOMO and LUMO energy levels of **P-DOTPA**



## 4. Photophysical characterization

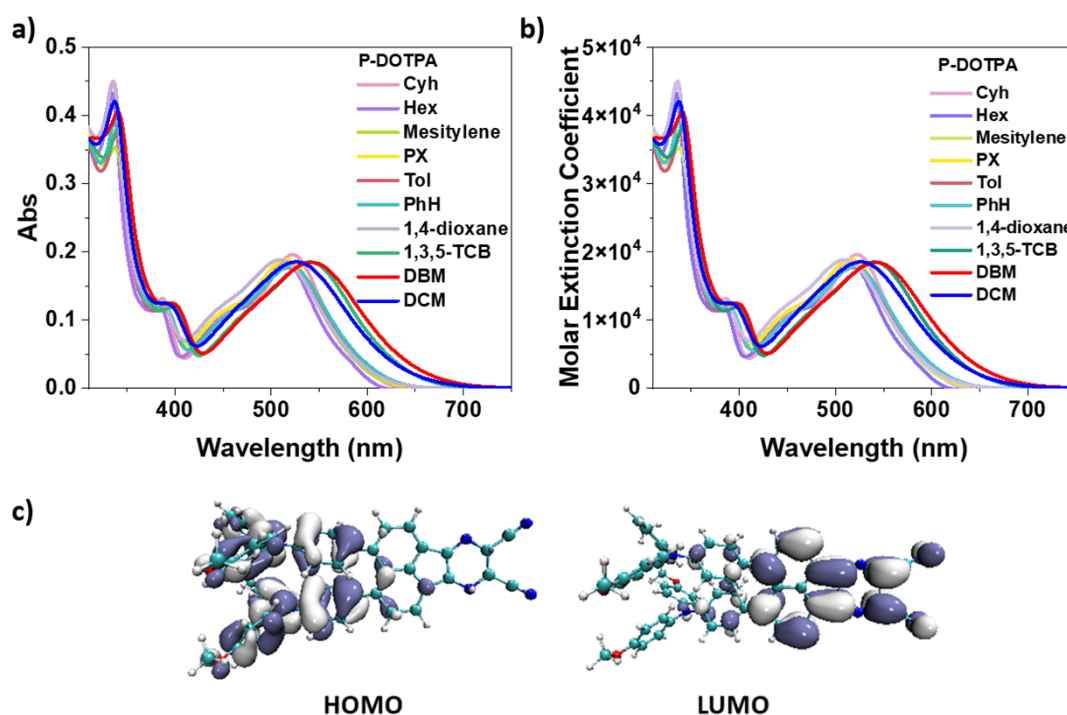


**Figure S2.** Absorption spectra (a) and molar extinction coefficient (b) of **P-DOTPA** (10  $\mu$ M) in different solvents. Hex: *n*-hexane; Cyh: cyclohexane; PX: 1,4-xylene; Tol: toluene; PhH: benzene; 1,3,5-TCB: 1,3,5-trichlorobenzene; DBM: dibromomethane; DCM: dichloromethane. c) The  $S_0$  state HOMO and LUMO electron distribution of **P-DOTPA**.

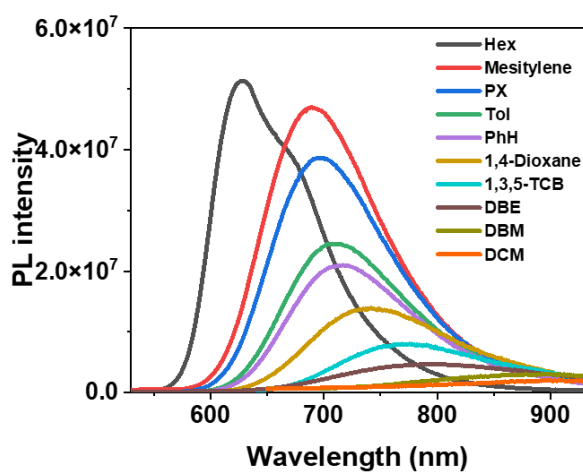


**Figure S3.** PL spectra of **P-DOTPA** (10  $\mu$ M) in different solvents.

## SUPPORTING INFORMATION

**Table S2.** The summarized **P-DOTPA** spectroscopic data for various solvents were presented.

Solvent	cyh	Hex	Mesitylene	PX	Tol	PhH	Diox	1,3,5-TCB	DMBA	DBE	DBM	DCM
$E_T(30)$ kcal/mol	30.9	31	32.9	33.1	33.9	34.3	36	36.2	36.5	38.3	39.4	40.7
$\lambda_{em}(nm)$	631	627	689	696	716	719	755	773	805	834	888	908
PLQY air	29.5%	26%	19.3%	18.6%	12%	10.5%	-	-	-	-	-	-

Note:  $E_T(30)$  is the polarity index from the literature (Chem. Rev. 1994, 94, 2319–2358).

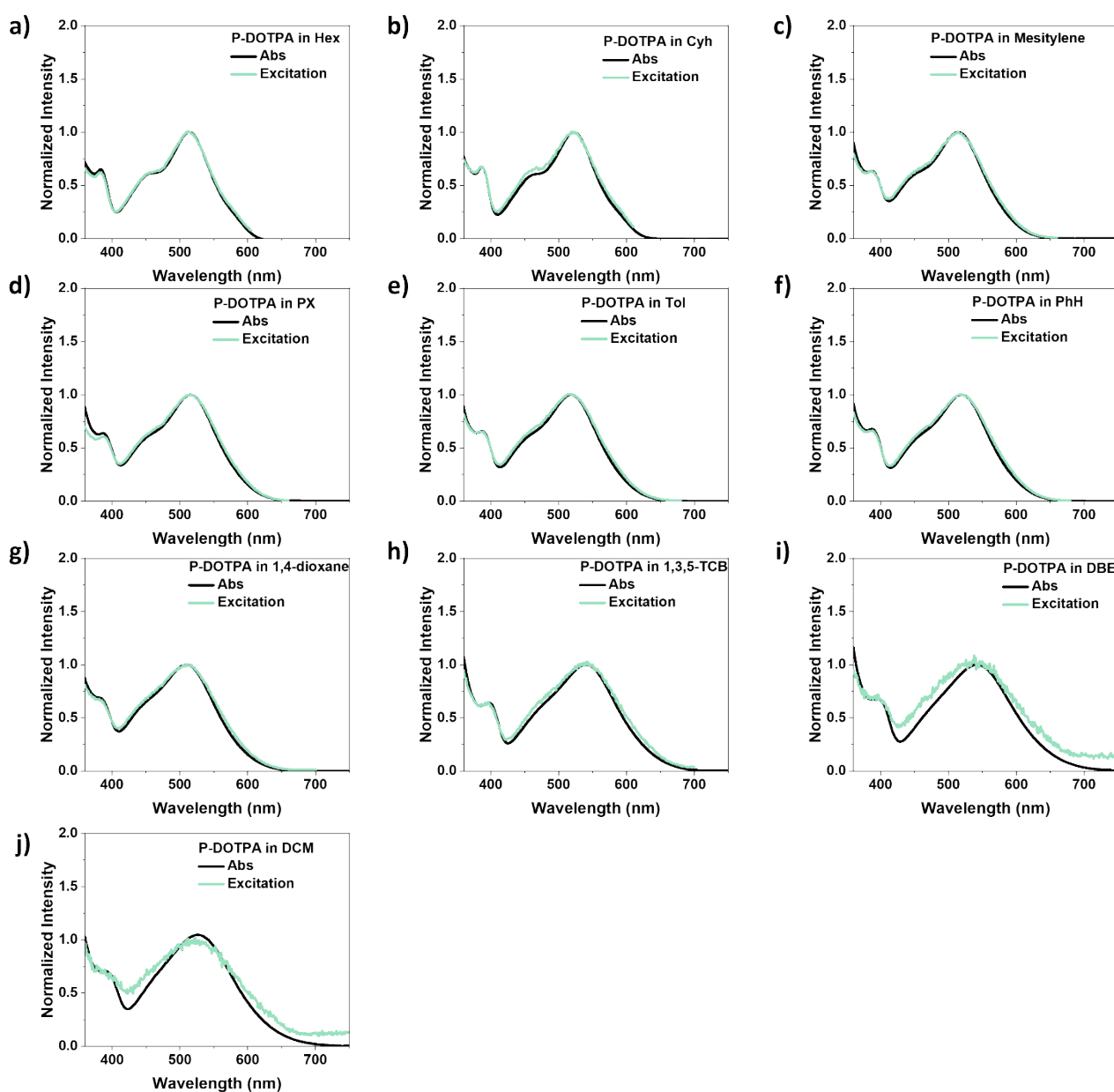


**Figure S4.** Absorption and excitation spectra of **P-DOTPA** in different solvents (10  $\mu$ M, excitation spectra monitored at corresponding emission maximum).

## SUPPORTING INFORMATION

**Table S3.** Solvent parameters of binary mixed solvents

NO.	Cyh Percent (Volume Fraction)	Tol Percent (Volume Fraction)	$\varepsilon_{mix}^a$	$n_{mix}^2{}^b$	$\Delta f^c$
1	10 %	90 %	0.23015	0.24325	0.10853
2	20 %	80 %	0.22063	0.25837	0.09144
3	30 %	70 %	0.21041	0.27181	0.0745
4	40 %	60 %	0.19941	0.28383	0.0575
5	50 %	50 %	0.18755	0.29465	0.04022
6	60 %	40 %	0.17471	0.30444	0.02249
7	70 %	30 %	0.16076	0.31333	0.0041
8	80 %	20 %	0.14557	0.32146	-0.01515
9	90 %	10 %	0.12896	0.3289	-0.03549

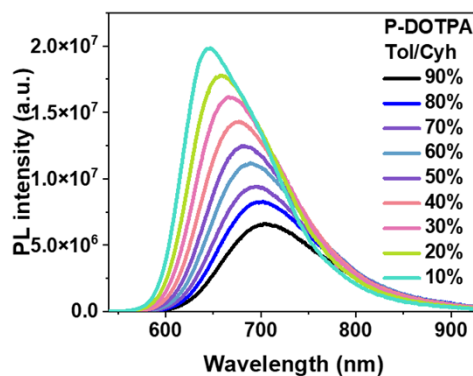
<sup>a</sup>Dielectric constant, <sup>b</sup>refractive indices, and <sup>c</sup>orientation polarizability of the mixture of Cyh and Tol, which are calculated from Eq. (S1), (S2), and (S3), where the subscripts a and b represent the two different neat solvents and c is the Lippert Mataga polarity parameter  $\Delta f$  of each solvent.

$$\varepsilon_{mix} = f_a \varepsilon_a + f_b \varepsilon_b \quad (S1)$$

$$n_{mix}^2 = f_a n_a^2 + f_b n_b^2 \quad (S2)$$

$$\Delta f = \frac{\varepsilon - 1}{2\varepsilon + 1} - 0.5 \frac{n^2 - 1}{2n^2 + 1} \quad (S3)$$

Preparation of the Cyh/Tol mixing system: A 25  $\mu$ L sample of the probe solution was removed and dissolved in different proportions of water and tetrahydrofuran. The resulting probe solution was then diluted to a concentration of 10  $\mu$ M. The magnitude of polarity can be calculated by substituting the values into the Lippert-Mataga equation.



## SUPPORTING INFORMATION

**Figure S5.** The PL spectra of **P-DOTPA** (10  $\mu$ M) in different ratios of TOL: Cyh mixed solvents.

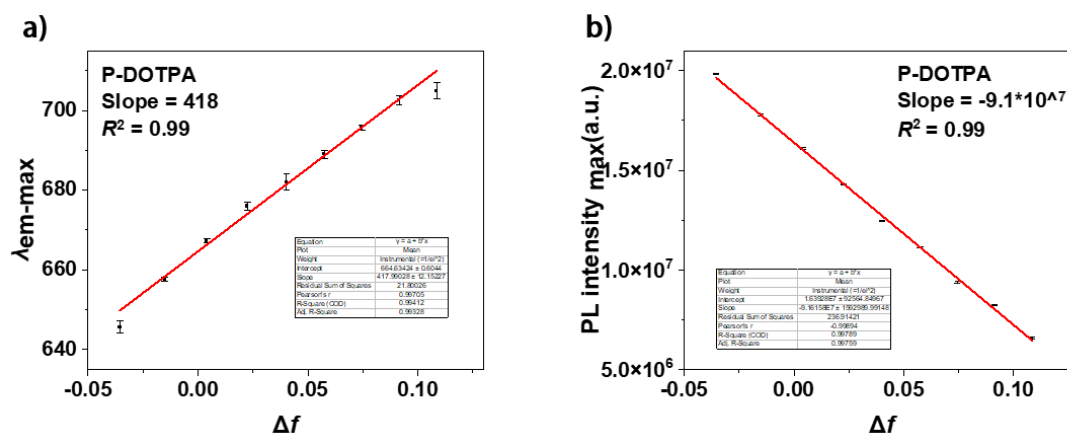


**Figure S6.** The linear relationship between emission wavelength and  $\Delta f$  of **P-DOTPA** (a) in different ratios of TOL: CYH mixed solvents. Linearity between  $I_{\max}$  and polarity  $\Delta f$  of **P-DOTPA** (b) in different ratios of TOL: CYH mixed solvents. Values were expressed as mean  $\pm$  SD ( $n = 3$ ).

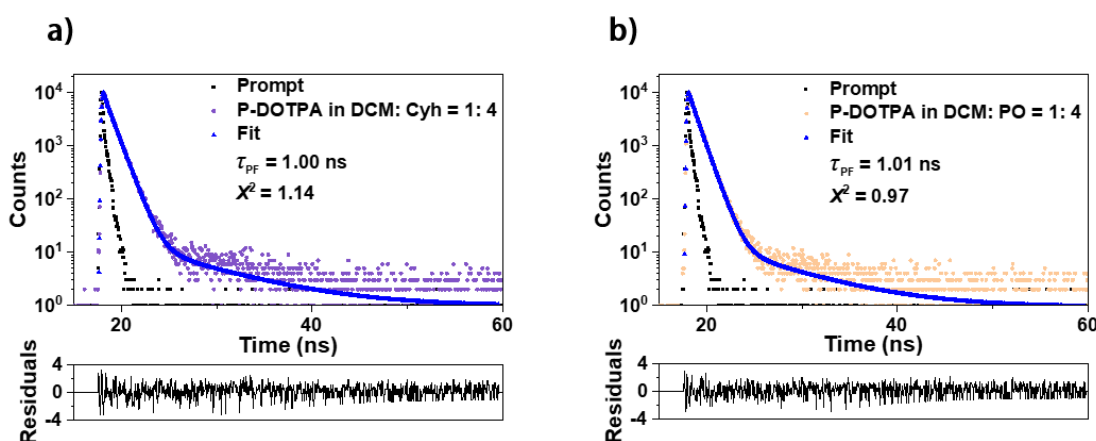


**Figure S7.** Experimental findings and fitting results of the PL decay profiles of **P-DOTPA** in an aerated binary solvent system at room temperature ( $\lambda_{\text{ex}} = 505$  nm,  $\lambda_{\text{em}} = 740$  nm). (a) 10  $\mu$ M in DCM: Cyh = 1: 4; (b) 10  $\mu$ M in DCM: PO = 1: 4.

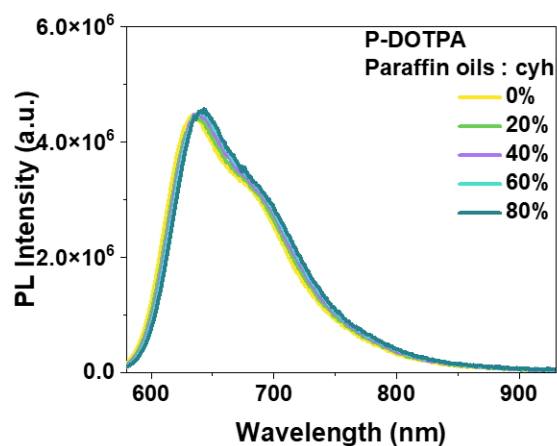


**Figure S8.** The Fluorescence response of probe **P-DOTPA** (10  $\mu$ M) to the paraffin oil/cyh mixed system (paraffin oil fraction from 0 to 80%; Cyh and paraffin oil have similar polarity but different viscosity).

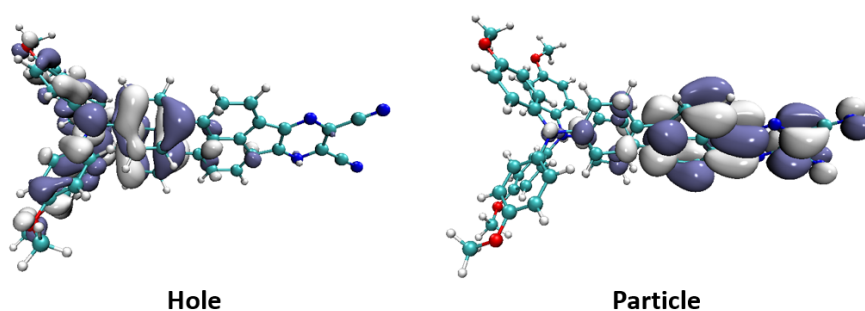


**Figure S9.** The  $S_1$  state hole and particle electron distribution of **P-DOTPA**.

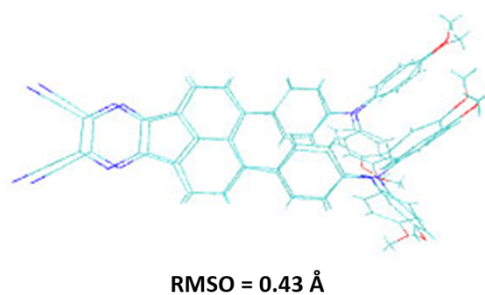


**Figure S10.** Calculate the RMSD between  $S_0$  and  $S_1$  state configurations of **P-DOTPA**,

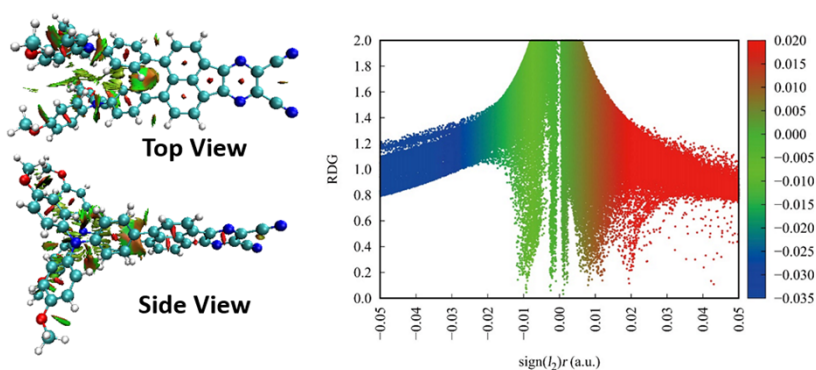


**Figure S11.** RDG scatter diagrams and RDG isosurface map of **P-DOTPA**.

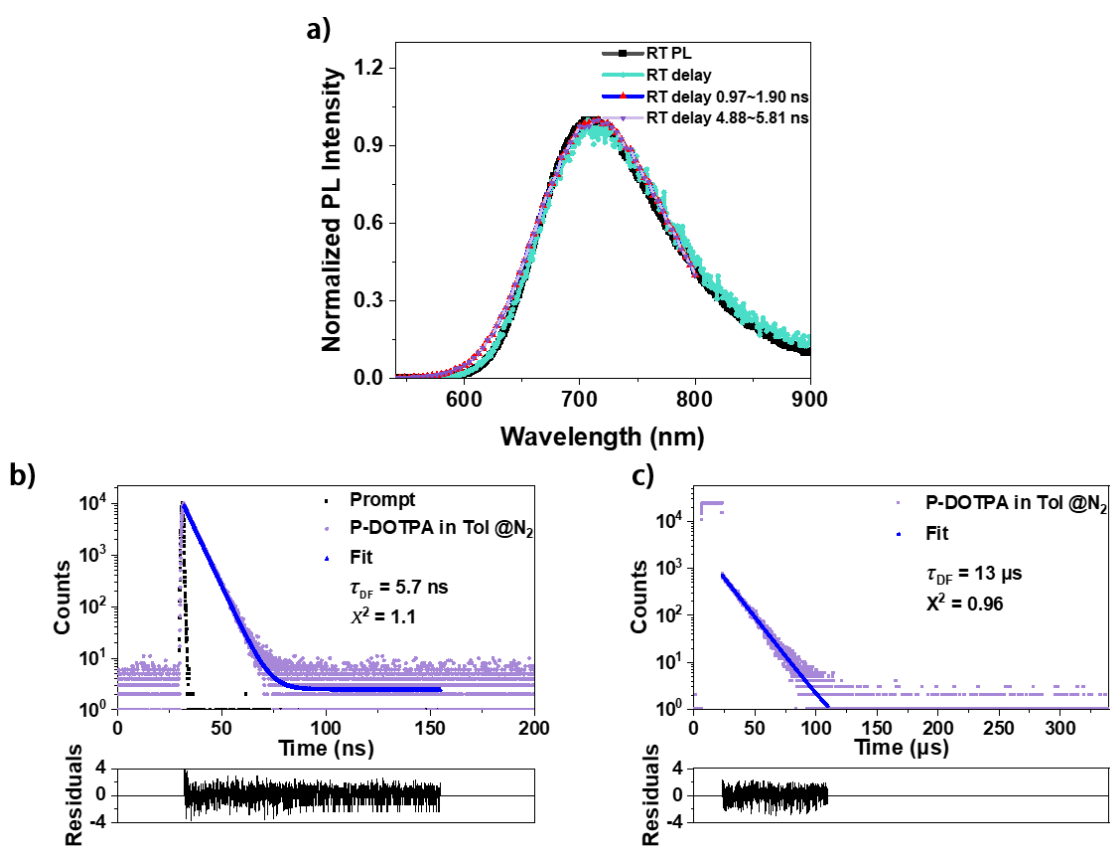


**Figure S12.** a) TRES spectra of **P-DOTPA** monitored at ns-scale and  $\mu$ s-scale in  $N_2$ -degassed Tol solution at RT ( $\lambda_{\text{ex}} = 505$  nm, 10  $\mu$ M). b-c) Experimental findings and fitting results of the PL decay profiles of 10  $\mu$ M **P-DOTPA** in an  $N_2$ -degassed Tol solution at room temperature ( $\lambda_{\text{ex}} = 505$  nm,  $\lambda_{\text{em}} = 716$  nm). (b) In a ns-scaled time window; (c) in a  $\mu$ s-scaled time window.

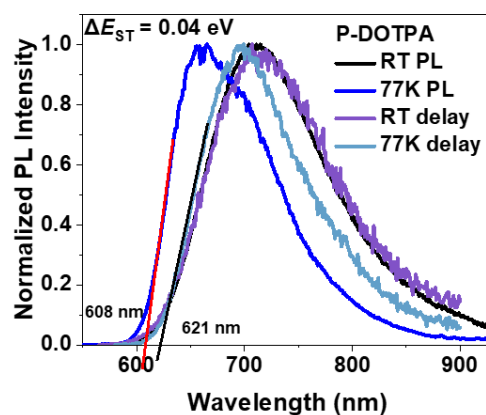


**Figure S13.** The Fluorescence spectra and delay spectra of **P-DOTPA** in toluene at room temperature and 77K ( $\lambda_{\text{ex}} = 505 \text{ nm}$ , 10  $\mu\text{M}$ ).

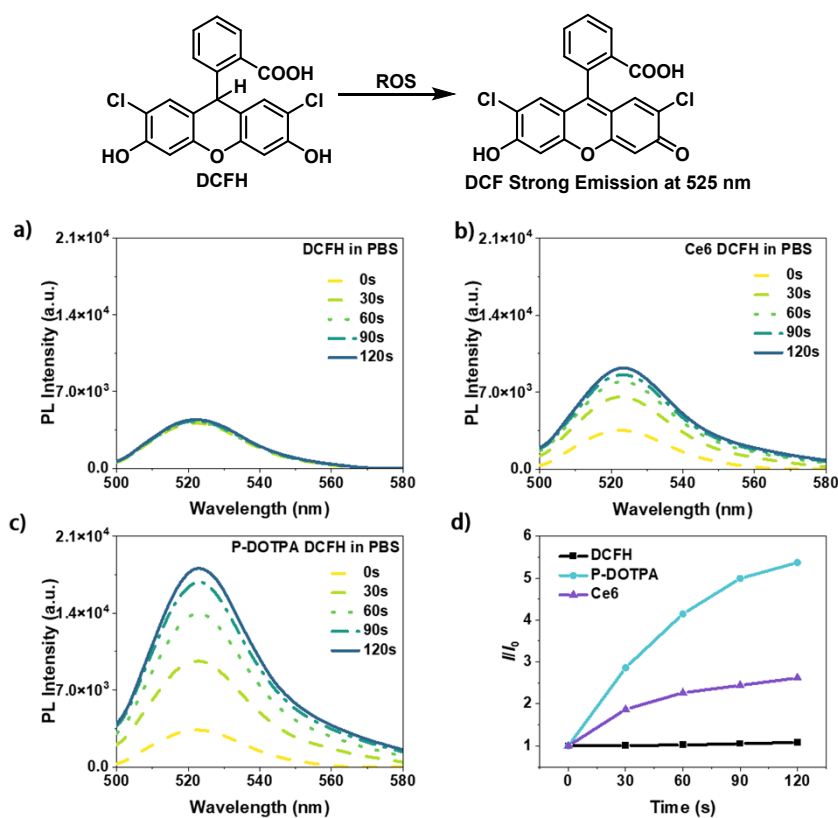


**Figure S14.** Fluorescence intensity of DCFH at 525 nm as a function of irradiation time (0-120 s) in the presence of DCFH (a), Ce6+DCFH (b), **P-DOTPA**+DCFH (c), and summarize the ratio of fluorescence intensity before and after illumination (c) in PBS.

## SUPPORTING INFORMATION

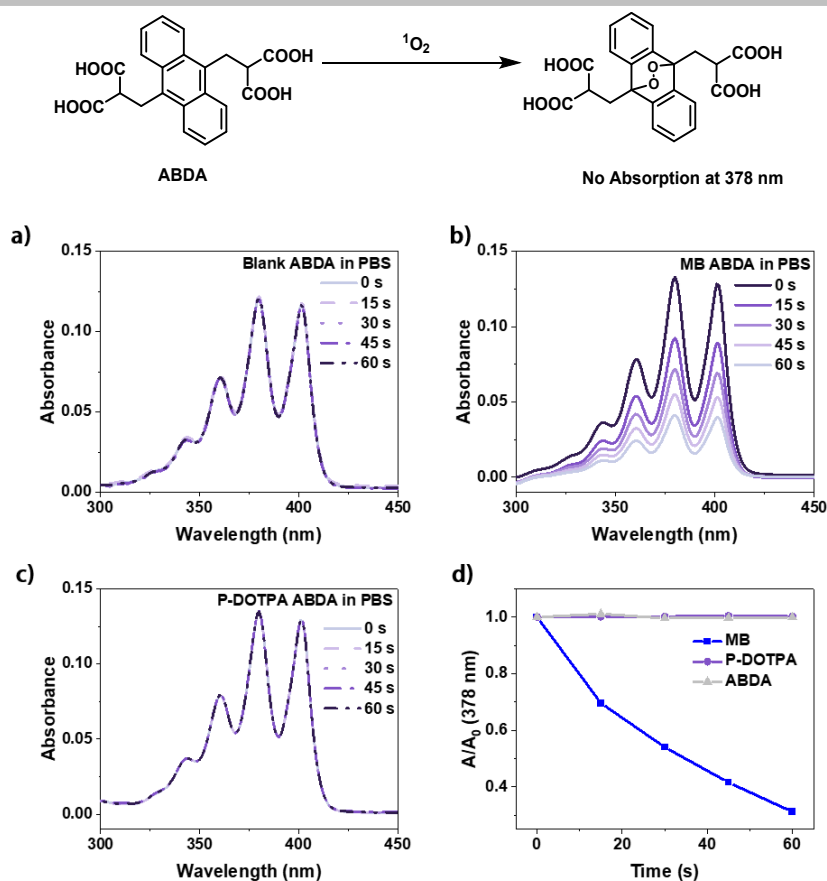


**Figure S15.** Absorption intensity of ABDA of irradiation time (0-90 s) in the presence of ABDA (a), MB+ABDA (c), and **P-DOTPA**+ABDA (c) in PBS.

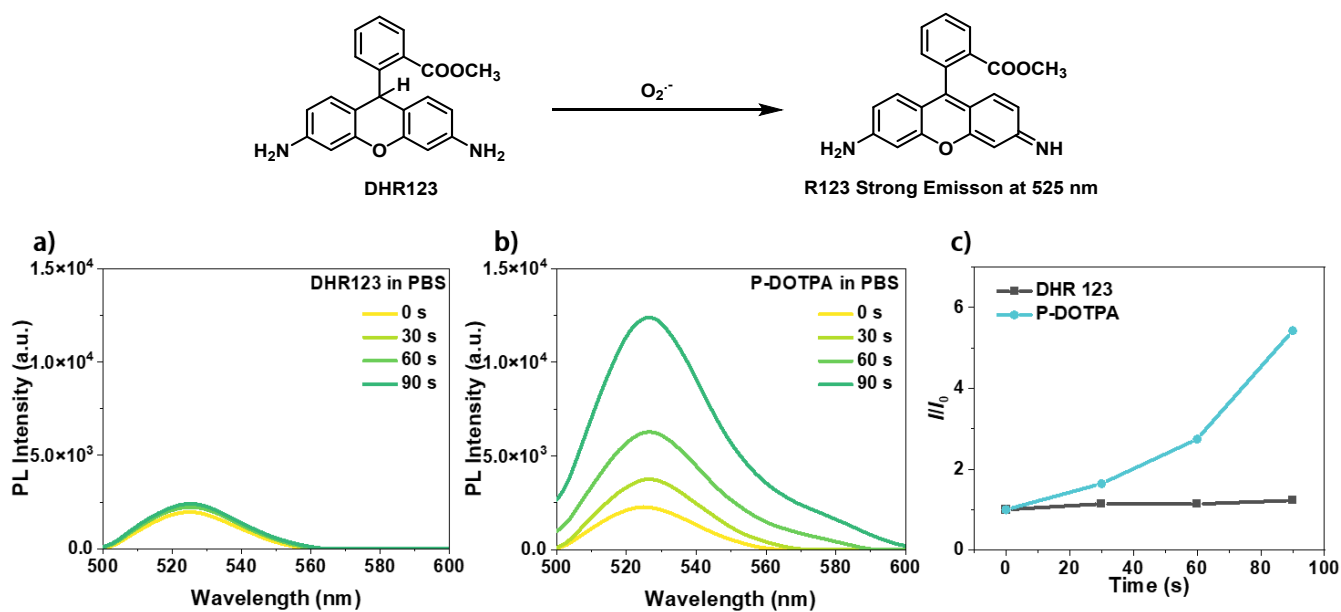


**Figure S16.** Fluorescence intensity of DHR123 at 525 nm as a function of irradiation time (0-90 s) in the presence of DHR123 (a), **P-DOTPA**+DHR123 (b), and summarize the ratio of fluorescence intensity before and after illumination (c) in PBS.



## SUPPORTING INFORMATION

### 5. Biological experiments

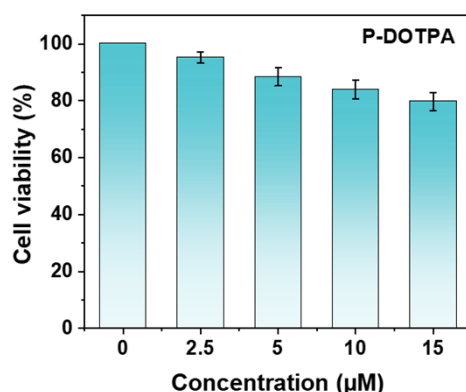


**Figure S17.** Cell viability of 4T1 cells after incubation with different concentrations of **P-DOTPA** (0–15 μM) after 24 h incubation. Values were expressed as mean ± SD (n = 6).

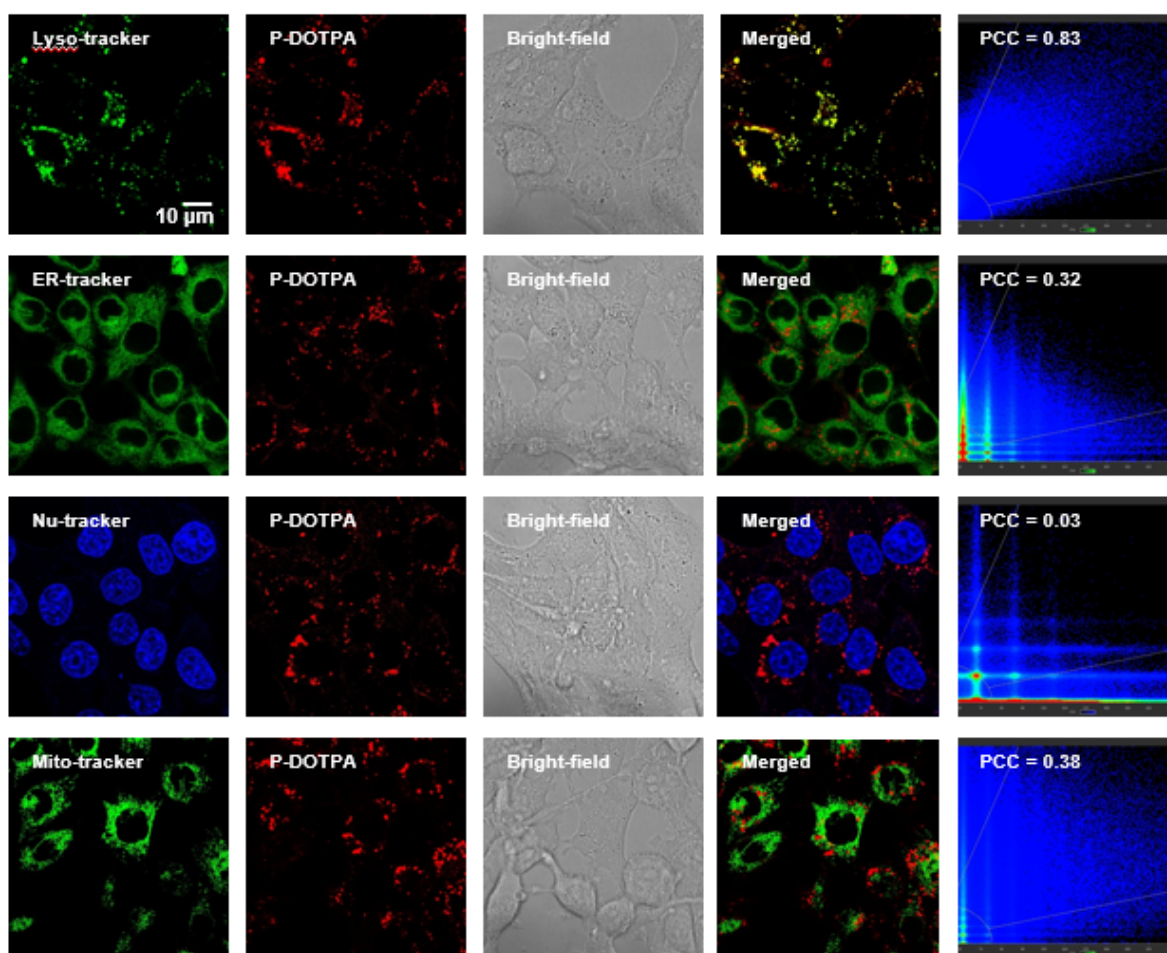


**Figure S18.** Confocal microscopy fluorescence images of 4T1 cells co-labeled with (10 μM) for **P-DOTPA** 4.5 h and commercial organelle trackers (10 μM) for 30 min: Lyso-tracker (0.2 μM,  $\lambda_{\text{ex}}/\lambda_{\text{em}} = 488/500\text{--}600$  nm). ER-tracker (0.2 μM,  $\lambda_{\text{ex}}/\lambda_{\text{em}} = 488/500\text{--}600$  nm). Nu-tracker (0.2 μM,  $\lambda_{\text{ex}}/\lambda_{\text{em}} = 405/420\text{--}500$  nm). Mito-tracker (0.2 μM,  $\lambda_{\text{ex}}/\lambda_{\text{em}} = 488/500\text{--}600$  nm). For **P-DOTPA** imaging:  $\lambda_{\text{ex}}/\lambda_{\text{em}} = 561/600\text{--}850$  nm.

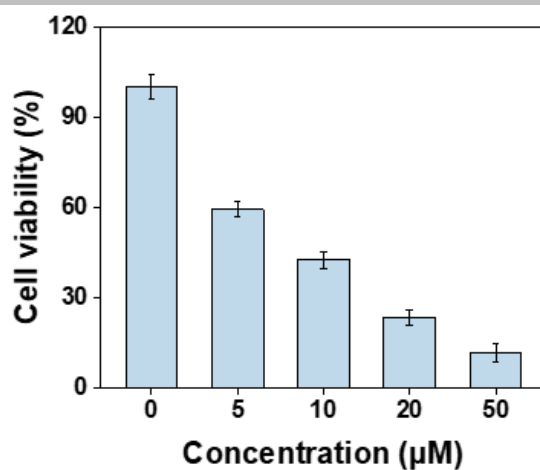


**Figure S19.** Cell viability was assessed after incubating 4T1 cells with different concentrations of P-DOTPA for 4.5 hours, followed by 10 minutes of light exposure. The results are expressed as mean  $\pm$  SD (n = 6).

## 6. $^1\text{H}$ NMR, $^{13}\text{C}$ NMR, and HRMS

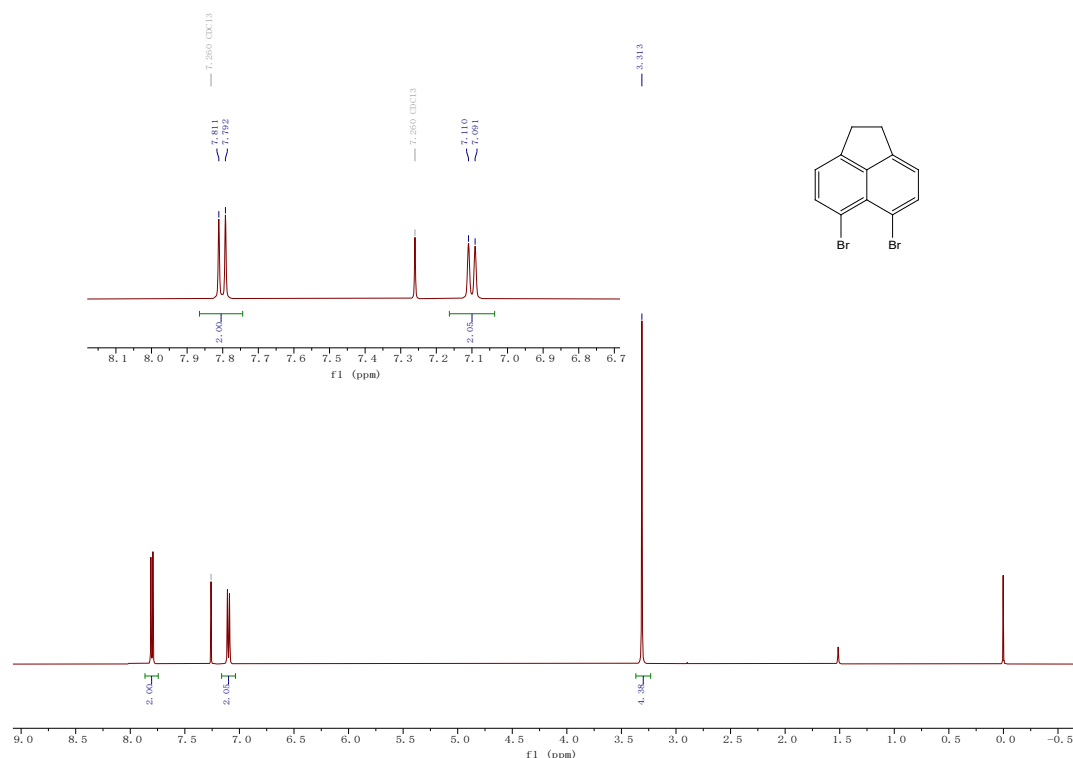
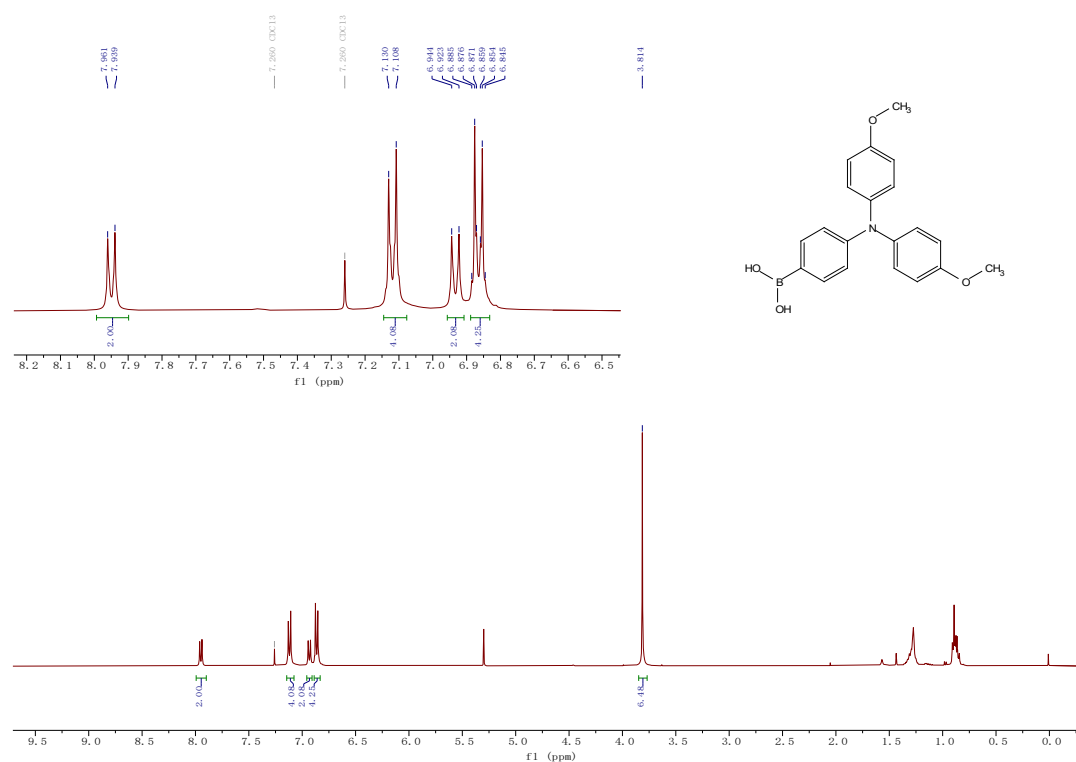
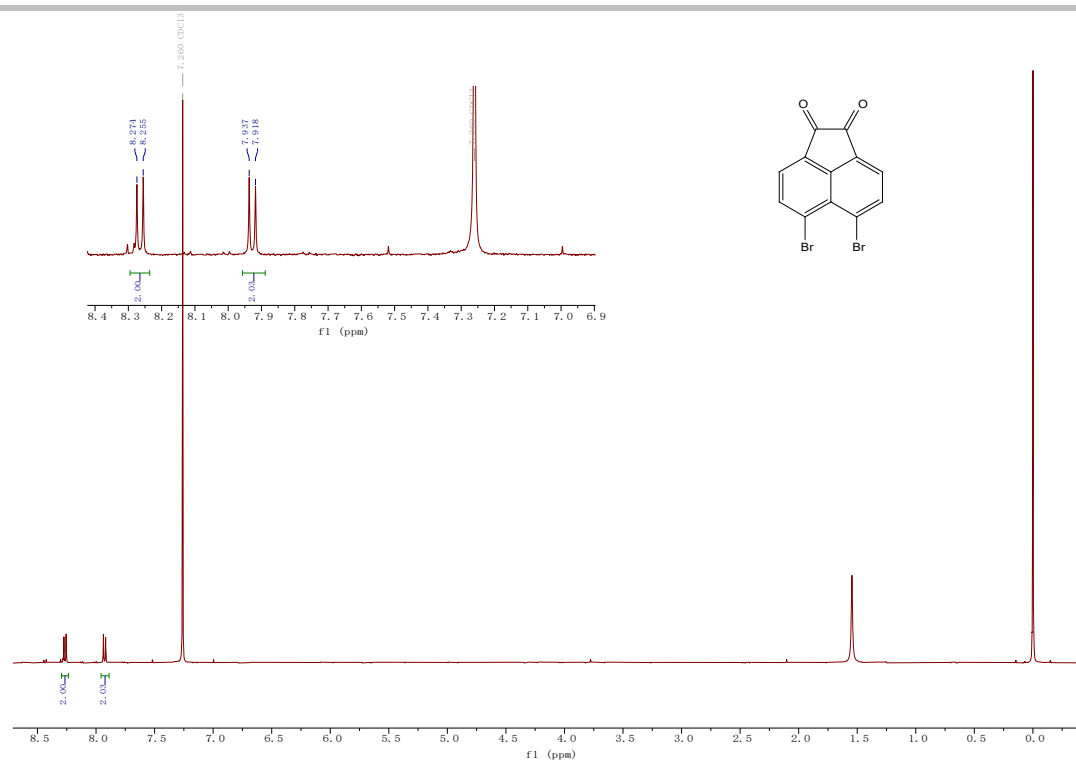


**Figure S20.** The  $^1\text{H}$  NMR spectrum of A2 in CDCl<sub>3</sub>.

# SUPPORTING INFORMATION



# SUPPORTING INFORMATION

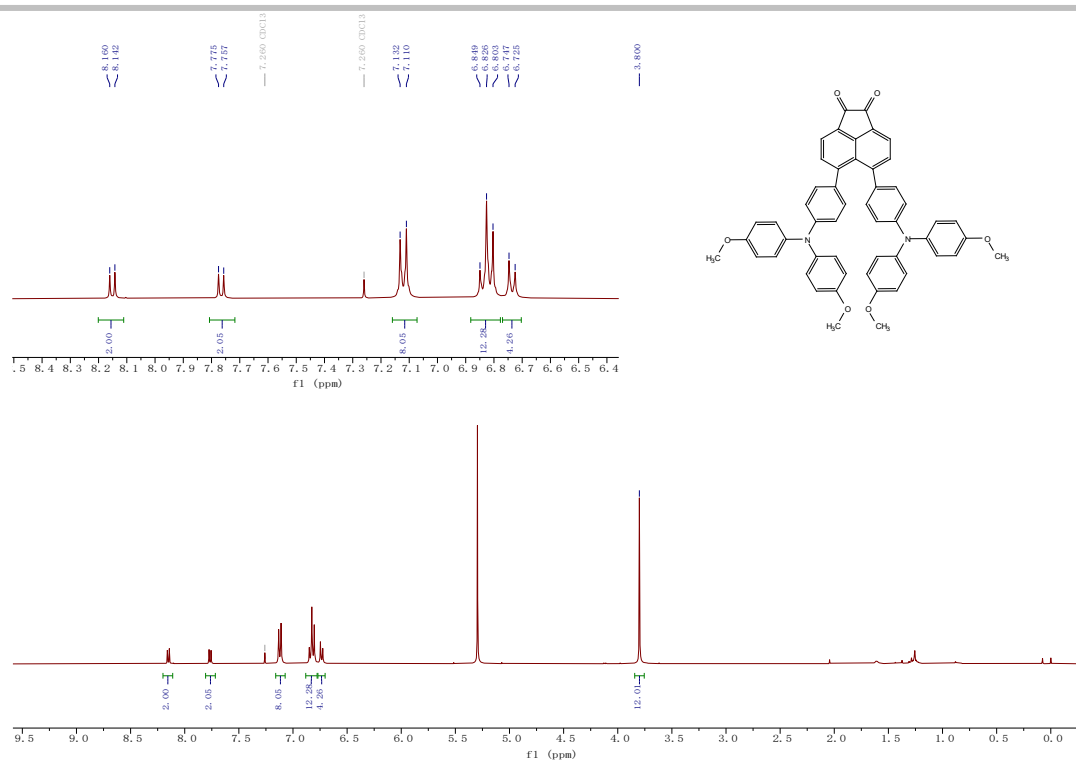


**Figure S23.** The  $^1\text{H}$  NMR spectrum of **P3** in  $\text{CDCl}_3$ .

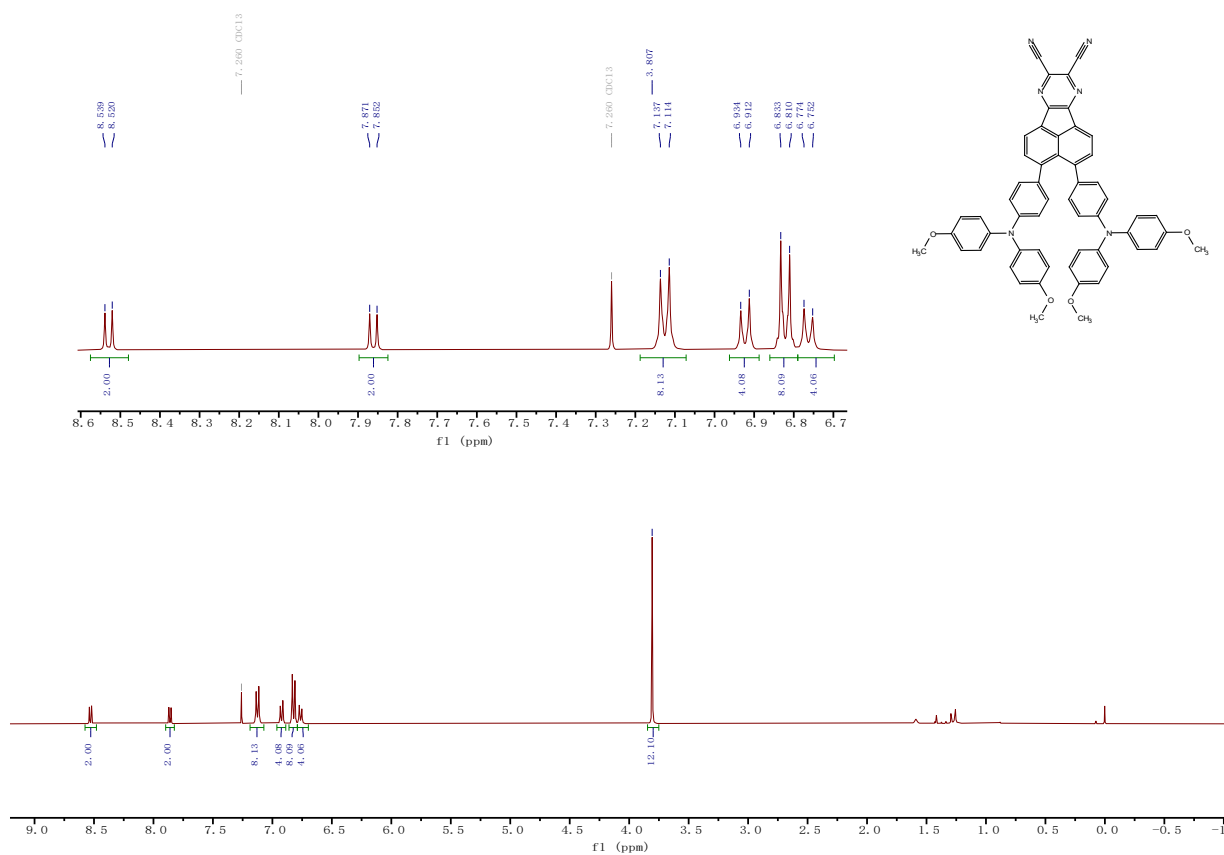


**Figure S24.** The  $^1\text{H}$  NMR spectrum of **P-DOTPA** in  $\text{CDCl}_3$ .

## SUPPORTING INFORMATION

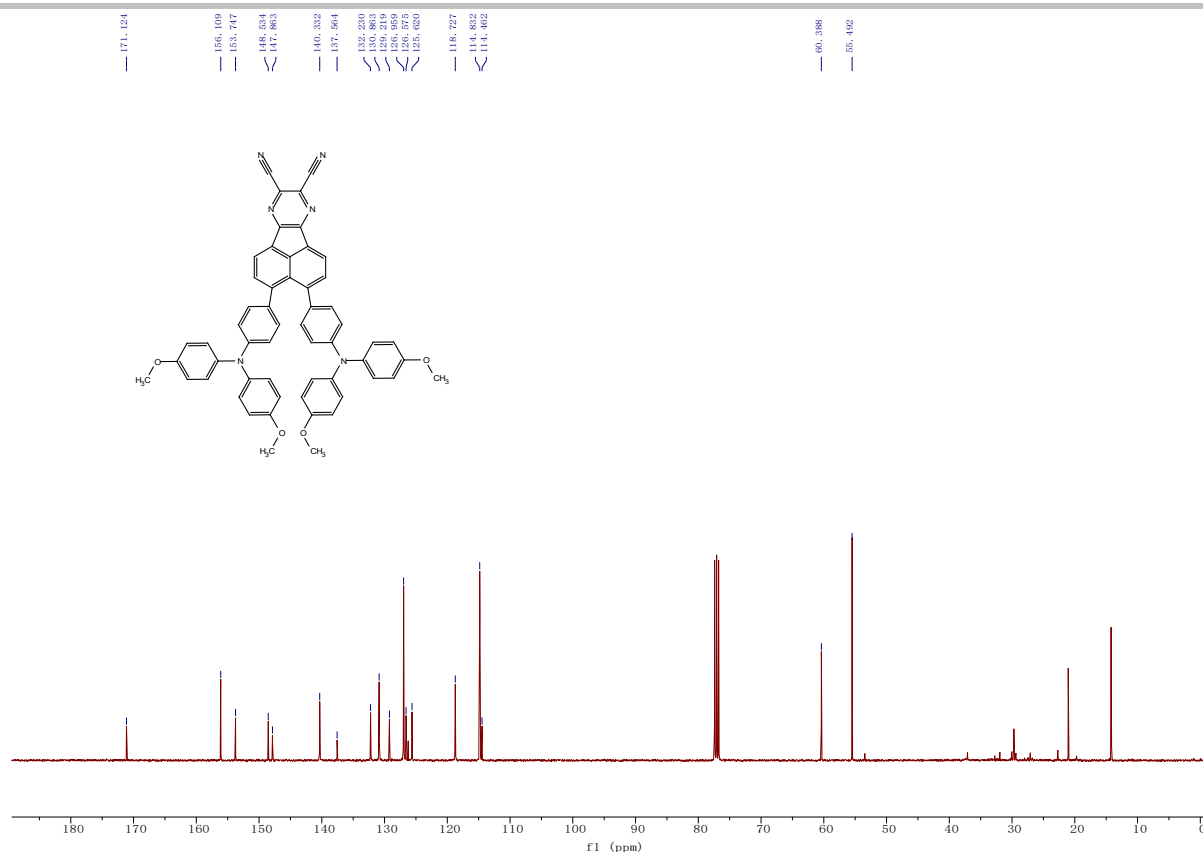


**Figure S25.** The  $^{13}\text{C}$  NMR spectrum of P-DOTPA in  $\text{CDCl}_3$ .

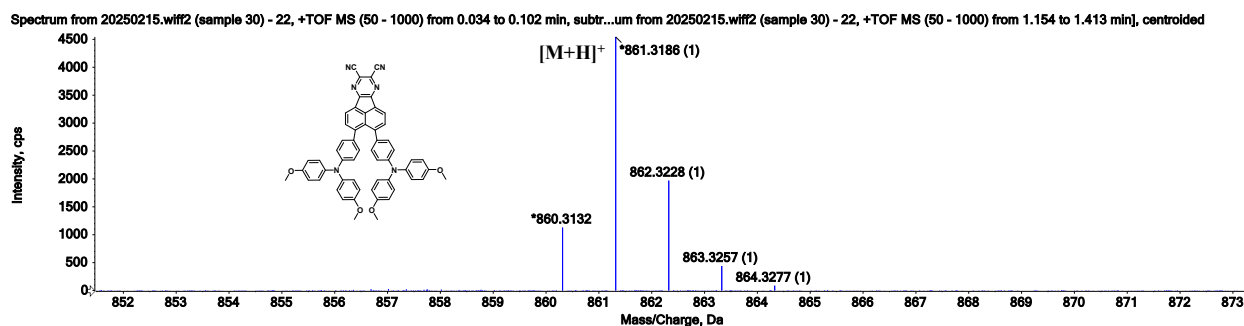


**Figure S26.** HRMS spectrum of P-DOTPA

## References

- [1] R. Huang, K. Yu, S. Chen, K. Chen, Y. Luo, Z. Lu, F. B. Dias and X. Zheng, *Advanced Optical Materials* **2024**, *12*.
- [2] C. Jin, P. Wu, Y. Yang, Z. He, H. Zhu and Z. Li, *Redox Biology* **2021**, *46*.
- [3] D. Shi, L. Hu, X. Li, W. Liu, Y. Gao, X. Li, B. Jiang, C. Xia, Y. Guo and J. Li, *Sensors and Actuators B: Chemical* **2020**, *319*.
- [4] Y. Dai, Z. Zhan, Q. Li, R. Liu and Y. Lv, *Analytica Chimica Acta* **2020**, *1136*, 34-41.
- [5] Y. Wang, G. Wang, K. Wang, Z. Wang, Y. Guo and H. Zhang, *Sensors and Actuators B: Chemical* **2018**, *261*, 210-217.

## SUPPORTING INFORMATION

---

- [6] L. Fan, X. Wang, J. Ge, F. Li, X. Wang, J. Wang, S. Shuang and C. Dong, *Chemical Communications* **2019**, 55, 4703-4706.
- [7] Z. Yuan, J. Chen, Q. Zhou, A. Liu, Z. Qiang, M. Fang, M. Chen, Y. Feng, H. Yu, X. Yang and X. Meng, *Chinese Chemical Letters* **2021**, 32, 1803-1808.
- [8] H. Zhu, J. Fan, H. Mu, T. Zhu, Z. Zhang, J. Du and X. Peng, *Scientific Reports* **2016**, 6.
- [9] X. Chen, W. Wang, T. Ye, J. Kang, Q. Wang, W. Yang, H. Dai, K. Wang and J. Pan, *Bioconjugate Chemistry* **2023**, 34, 1851-1860.
- [10] J. Zhang, S. Gong, Q. Li, S. Zhang and G. Feng, *Analytical Chemistry* **2024**.
- [11] T. Wu, L. Duan, J. Yang and Y. Zhou, *Sensors and Actuators B: Chemical* **2023**, 393.
- [12] J. Jiang, X. Tian, C. Xu, S. Wang, Y. Feng, M. Chen, H. Yu, M. Zhu and X. Meng, *Chemical Communications* **2017**, 53, 3645-3648.
- [13] Q. Hu, H. Zhang, P. Ye, S. Ma, X. Zhu and Y. Bai, *Dyes and Pigments* **2023**, 208.
- [14] J. Yin, M. Peng and W. Lin, *Chemical Communications* **2019**, 55, 11063-11066.
- [15] W.-L. Jiang, Z.-Q. Wang, Z.-K. Tan, G.-J. Mao, J. Fei and C.-Y. Li, *Journal of Materials Chemistry B* **2022**, 10, 4285-4292.
- [16] K. Pal, P. Kumar and A. L. Koner, *Journal of Photochemistry and Photobiology B: Biology* **2020**, 206.